Environmental Modelling & Software 76 (2016) 54–68

Contents lists available at ScienceDirect

Environmental Modelling & Software

journal homepage: www.elsevier.com/locate/envsoft

WRF-LTNGDA: A lightning data assimilation technique implemented in the WRF model for improving precipitation forecasts

Theodore M. Giannaros*, Vassiliki Kotroni, Konstantinos Lagouvardos

National Observatory of Athens, Institute for Environmental Research and Sustainable Development, Vas. Pavlou & Metaxa, 15236, Athens, Greece

ARTICLE INFO

Article history:
Received 13 March 2015
Received in revised form
20 November 2015
Accepted 24 November 2015
Available online 11 December 2015

Keywords:
Data assimilation
Lightning
WRF
Convection parameterization scheme
Precipitation prediction
Greece

ABSTRACT

This study introduces WRF-LTNGDA, a lightning data assimilation technique implemented in the Weather Research and Forecasting (WRF) model. This technique employs lightning for improving the representation of convection by means of controlling the triggering of the model's convection parameterization scheme. The development and implementation of WRF-LTNGDA was carried out in a framework that could easily allow for its exploitation in real-time forecasting activities. The assimilation algorithm was evaluated over eight precipitation events that took place in Greece in the years 2010–2013. Results clearly show that lightning forcing has a positive impact on model performance. The conducted analysis revealed that the employment of WRF-LTNGDA induces statistically significant improvements in precipitation verification scores, especially for high rainfall accumulations. Separate examination of one of the eight case studies highlighted the overall better agreement between the modelled and observed spatial distribution of precipitation when lightning data assimilation was applied, than in the control simulation.

Software availability

Software name: WRF-LTNGDA
Developers: Theodore M. Giannaros, Vassiliki Kotroni, Konstantinos Lagouvardos
Contact address: National Observatory of Athens, Institute for Environmental Research and Sustainable Development, Vas. Pavlou & I. Metaxa, 15236, Athens, Greece
Email/Tel.: thgian@noa.gr, +30 210 8109203
Hardware required: Any Linux-based PC
Software required: Weather Research and Forecasting (WRF) model, version 3.5.1 or higher
Program language: Fortran
Availability and cost: Currently provided freely through personal communication with the developers.

1. Introduction

It has well been documented that the success of a numerical simulation depends heavily on the accuracy with which the true atmospheric state is represented at the time of model initialization. This accuracy can be achieved through data assimilation. For instance, Carvalho et al. (2012) demonstrated that the implementation of a simple nudging scheme in the Weather Research and Forecasting (WRF) model can provide better wind predictions. Van Loon et al. (2000) used the Ensemble Kalman Filter approach to assimilate ozone in the chemistry transport model LOTOS, while a sequential emulator-based assimilation scheme was implemented by Margvelashvili et al. (2013) in a 3D coastal sediment transport model. More recently, Peters-Lidard et al. (2015) presented a WRF-based integrated land-atmosphere modeling system that exploits the latest techniques for assimilating a variety of observational data.

The development and implementation of lightning data assimilation techniques in numerical weather prediction (NWP) models have been attracting significant scientific effort during the past few years (Alexander et al., 1999; Papadopoulos et al., 2005, 2009; Mansell et al., 2007; Pessi and Businger, 2009; Fierro et al., 2012, 2014; Lagouvardos et al., 2013; Lynn et al., 2015). This effort is primarily driven by the necessity to provide more accurate predictions for convective precipitation, which is often associated with flash floods resulting in significant loss of life and property damages. The selection of lightning is justified since it has been widely recognized as a valuable proxy variable for identifying the

* Corresponding author.
E-mail address: thgian@noa.gr (T.M. Giannaros).

http://dx.doi.org/10.1016/j.envsoft.2015.11.017
1364-8152/

occurrence of severe convection (Schultz et al., 2011), relating well with convective precipitation (Goodman et al., 1988; Zhou et al., 2002; Gauthier et al., 2006).

Several different techniques have been proposed for the ingestion of lightning data into NWP models, aiming to tackle the well-documented spin-up problem (e.g. Davidson and Puri, 1992) due to inadequate determination of moisture and divergence fields in initial conditions. The study of Alexander et al. (1999) is considered to be the first one to report on the positive feedback of lightning data assimilation on 12–24 h precipitation forecasts. In this study, lightning data were used for deriving rainfall rates that were, consequently, assimilated in the meteorological model for simulating an extra-tropical cyclone. Chang et al. (2001) followed a similar approach a couple of years later. Mansell et al. (2007) modified the Kain–Fritsch (Kain and Fritsch, 1993) convective parameterization scheme (CPS) in the Coupled Ocean-Atmosphere Mesoscale Prediction System (COAMPS) mesoscale model (Hodur, 1997) to enable the use of lightning data for controlling the "trigger" function of the CPS. Lagouvardos et al. (2013) also implemented a similar technique in their simulations of a heavy precipitation event with the MM5 model (Dudhia, 1993). Papadopoulos et al. (2005, 2009) made use of lightning data to force deep moist convection in a mesoscale model by nudging the modelled humidity profiles towards empirical profiles derived from observations during thunderstorm days. More recently, Fierro et al. (2012) and Qie et al. (2014) presented two lightning data assimilation techniques that can perform at cloud-resolving scales, by means of modifying the microphysics parameterization scheme of the Weather Research and Forecasting (WRF) model (Skamarock et al., 2008).

The present study employs a mesoscale meteorological model and a lightning data assimilation technique very similar to those used in Mansell et al. (2007) and Lagouvardos et al. (2013), which are conceptually based on the earlier work of Rodgers et al. (2000) focusing on the assimilation of radar data. In this context, lightning data from a ground-based long-range detection network are used to control the triggering of a CPS during a prescribed assimilation period ending up to the forecast period. As highlighted by Mansell et al. (2007), the primary objective of this technique is to utilize lightning data to enable the activation or deactivation of subgrid-scale moist, deep convection during the assimilation period. This is expected to induce improvements on the representation of the mesoscale environment in the model, especially in cases when past convection has modified the environment by means of generating outflow boundaries and mesoscale upper-tropospheric outflow plumes (anvils).

The presented lightning data assimilation technique has been already tested in the COAMPS and MM5 models, showing promising results with regards to improving the simulation of precipitation (Mansell et al., 2007; Lagouvardos et al., 2013). However, both past studies were based on the investigation of a single precipitation event. This significantly influences the credibility of their results since the statistical significance of the changes induced by the assimilation technique on model performance has not been verified. In addition, Mansell et al. (2007) and Lagouvardos et al. (2013) employed large data assimilation time windows (i.e. 24 h and 18 h, respectively) that could hardly support operational readiness in a weather forecasting system.

Considering the above, this study presents a different framework for the evaluation of the impact of lightning data assimilation on precipitation forecast. The presented technique is implemented in the WRF model (Skamarock et al., 2008) and is evaluated over eight precipitation events that took place in Greece from 2010 to 2013. An advanced statistical significance test is consequently employed to ensure that the reported results are statistically tested. Further, a realistic assimilation time window is adopted, allowing for the examination of the capacity of the assimilation technique in terms of supporting operational weather forecasting applications.

2. Methodology

2.1. The assimilation technique

The technique for lightning data assimilation is based on the work of Mansell et al. (2007), as adapted by Lagouvardos et al. (2013). This technique employs lightning observations for controlling the activation of the CPS, which in the present study is the Kain–Fritsch (KF) scheme (Kain and Fritsch, 1993). This particular CPS has been selected instead of its newer version (Kain, 2004) due to its proven and well-documented capacity in terms of representing convection in the study area (e.g. Kotroni and Lagouvardos, 2001, 2004; Mazarakis et al., 2009). Further, the implemented lightning data assimilation technique has been originally developed and preliminary tested using the "old" KF scheme (Rodgers et al., 2000; Mansell et al., 2007; Lagouvardos et al., 2013).

The decision process tree of the assimilation technique is presented in Fig. 1. The lightning data assimilation procedure is called for each grid column of the model at 10 min intervals of integration time, checking the activation of the KF scheme. If the KF scheme is (not) active and lightning is (not) observed, then no action is taken. On the other hand, if the KF scheme has not been activated but lightning is observed, then the data assimilation algorithm decides whether or not it should be activated. Similarly, if the KF scheme has been activated but lightning is not observed, the algorithm decides, based on what the user requires, whether or not it should be suppressed.

The procedure used for triggering the KF scheme, when the latter is not active and lightning is observed, is described in detail in Mansell et al. (2007) and Lagouvardos et al. (2013). Briefly, the data assimilation algorithm begins with forcing the model layer of air most likely to coincide with the source of convection to its level of free convection (LFC). The capacity of this forcing in terms of allowing the KF scheme to produce a cloud at least 3 km deep is consequently checked. If such a cloud cannot be produced, then moisture is added to the parcel source layer by increments of 0.1 g kg^{-1}, up to 1 g kg^{-1}, aiming to force the formation of a convective cloud at least 3 km deep. If this is not achieved, the effort to trigger the KF scheme is abandoned.

For the case in which no lightning is observed, the data assimilation algorithm provides two options: (i) total suppression of the KF scheme, and (ii) no suppression at all (i.e. normal trigger of the KF scheme). If adopted, the first option results to skipping the KF scheme in all model grid points where no lightning activity is observed. Conversely, the second option results to a normal implementation of the KF scheme, even for those model grid points where lightning is not observed. The decision to incorporate these two options in the lightning data assimilation technique is based on the study of Mansell et al. (2007), who concluded that, depending on the case, either of the options might be appropriate.

2.2. Data sources

Lightning observations were provided by ZEUS, a long-range lightning detection network operated by the National Observatory of Athens (NOA) (Kotroni and Lagouvardos, 2008; Lagouvardos et al., 2009). ZEUS is capable of locating the source of very low frequency (VLF) radio emissions produced by cloud-to-ground (CG) and, secondarily, by strong intra-cloud (IC) lightning strikes, but it cannot distinguish between the two of them. The location accuracy of the network is approximately 6 km, while its detection efficiency

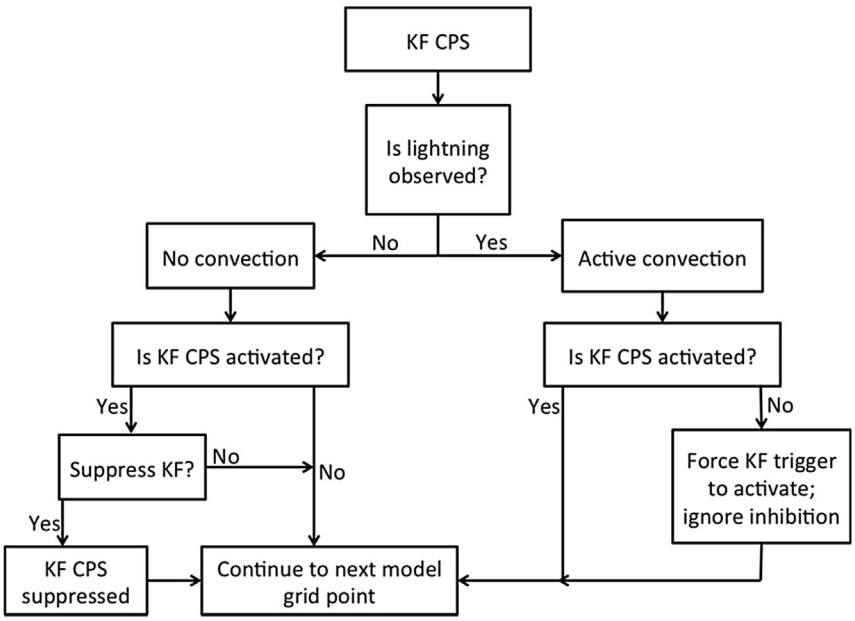

Fig. 1. Schematic representation of the decision process followed by the lightning data assimilation technique. Adapted from Lagouvardos et al. (2013).

equals ~25%.

The ZEUS network provides point data that need to be gridded in order to be used by the lightning data assimilation technique. For this, the observed lightning data are gridded to a 2D array matching the dimensions of the adopted model grid configuration (Sec. 2.3). Data are aggregated at 10 min intervals over a 6 h period, with each lightning impact simply incrementing the count in the model grid box in which it falls. The selection of the 10 min period for accumulating lightning observations is based on previous studies (Mansell et al., 2007; Lagouvardos et al., 2013), where a similar interval was employed to allow for alleviating the patchiness resulting from gridding the original point data.

Given the temporal resolution of the gridded lightning data, the KF scheme was set up to perform at the same time interval (i.e. "called" by the model every 10 min of integration time). The control of the scheme was consequently conducted on the basis of observed lightning activity within 10 min prior and 20 min after each model time step (i.e. employ three 10 min periods for controlling the activation of the KF scheme). This particular time window was adopted to allow for including the cases where convection may have initiated with lightning occurring later on, but no later than 20 min ahead of the considered time step. The threshold used for defining the occurrence of lightning activity is 1 lightning count per model grid cell, which is considered to be sufficient considering the location accuracy and detection efficiency of ZEUS.

2.3. Model setup

The lightning data assimilation technique was developed for and implemented in version 3.5.1 of the WRF model (Skamarock et al., 2008). For the current study, two 1-way nested modelling domains were specified with horizontal grid resolution of 24 km (DO1; mesh size of 185 × 125) and 6 km (DO2; mesh size of 181 × 173), as shown in Fig. 2a. The outermost domain (DO1) is used for simulating synoptic-scale atmospheric motions, while the innermost domain (DO2) focuses on the study area. In the vertical, 28 unevenly spaced sigma levels, up to 100 hPa, were defined for both domains.

Short-wave and long-wave radiation processes were parameterized with the Dudhia (Dudhia, 1989) and RRTM (Mlawer et al., 1997) schemes, respectively. For the planetary boundary layer, the Mellor–Yamada–Janjic (MYJ) parameterization (Janjic, 1994) was selected, coupled to the Eta similarity parameterization (Janjic, 1996, 2002) for the surface layer. Microphysics processes were parameterized with the Thompson scheme (Thompson et al., 2008), while Noah (Chen and Dudhia, 2001) was defined as the land-surface model. The KF CPS (Kain and Fritsch, 1993) was enabled on both domains, with lightning data assimilation also conducted in both domains.

2.4. Numerical experiments

To evaluate the performance of the lightning data assimilation technique, numerical experiments were conducted for eight events observed in the period 2010–2013 (Table 1). The events were selected to represent cases with widespread lightning activity and high precipitation amounts observed in the study area. For all events, WRF was initiated at 1200Z of the first day using the 6-hourly, 1 × 1 spatial resolution operational atmospheric analysis surface and upper air data provided by the National Centre for Environmental Predictions (NCEP). Daily high-resolution (i.e. 0.083 × 0.083) sea-surface temperature analyses, provided by NCEP, were also used for initializing the model. The duration of each numerical simulation was set to 30 h, and the interval for outputting data equaled 1 h.

For each of the selected events (Table 1), three numerical experiments were conducted, resulting to 24 simulations in total. The experiments marked with "CNTL" refer to the control WRF simulations with no lightning data assimilation. Experiments denoted with "LTNGDA" refer to WRF simulations with lightning data assimilation activated and the KF scheme being suppressed when lightning was not observed. Last, experiments denoted with "LTNGDA_NS" are similar to LTNGDA experiments, except for that the KF scheme is not being suppressed. Assimilation of lightning data was carried out for the first 6 h of each simulation (hereafter referred to as the "assimilation period") at 10 min intervals. The remaining 24 h of the simulation (hereafter referred to as the "forecast period") were used for the evaluation of the data

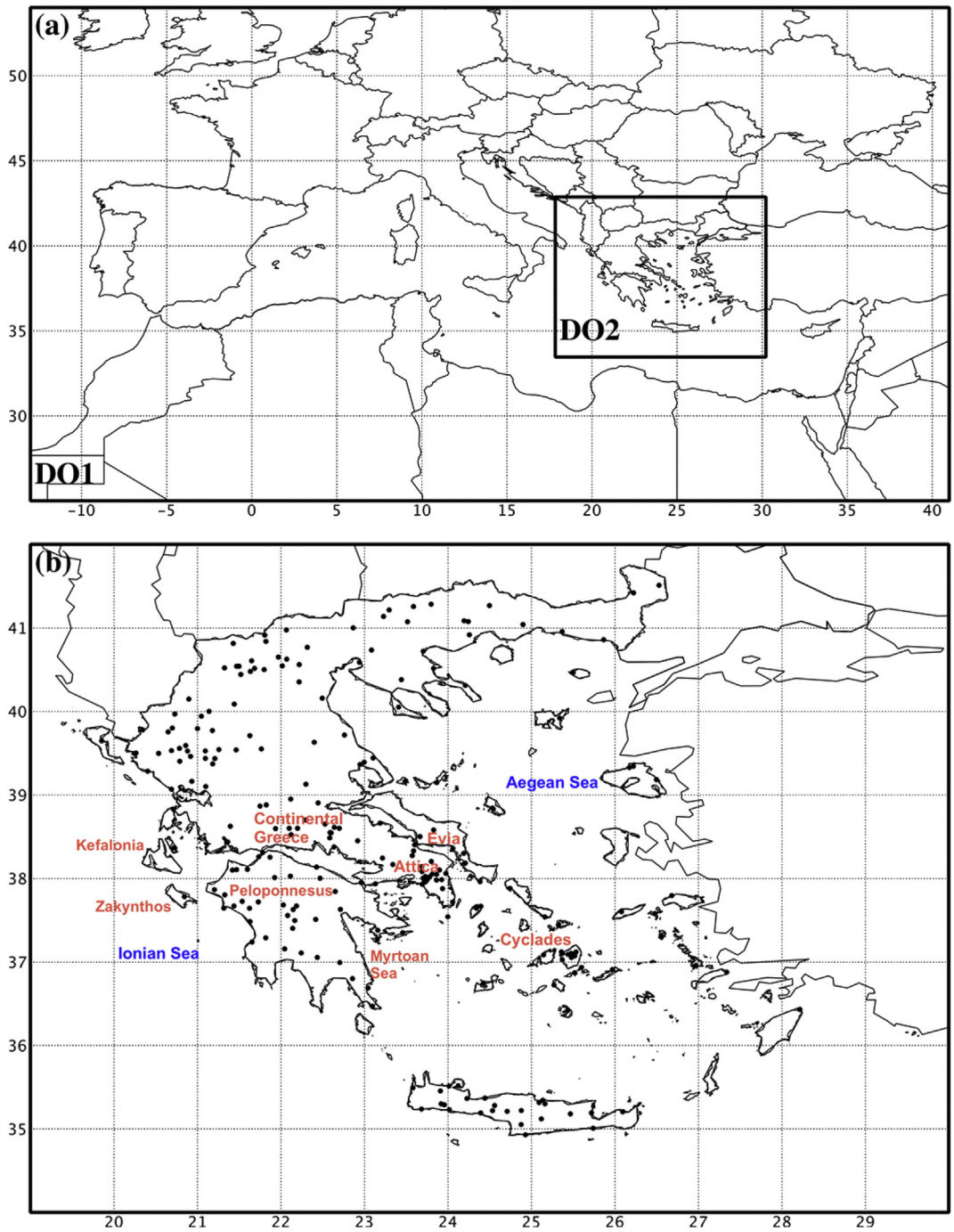

Fig. 2. (a) The WRF modelling domains used in this study. (b) Locations of the rain gauges (black circles) used for the verification of precipitation with identification of geographical areas of interest (text).

assimilation technique.

At this point it is worth justifying the selection of the duration (i.e. 6 h) for implementing the lightning data assimilation technique in the numerical simulations. As highlighted in Sec. 1, the primary objective of this study can be summarized in the evaluation of the lightning data assimilation in terms of its capacity for supporting real-time weather forecasting applications. To achieve this goal, it was necessary to define a realistic assimilation window that could be adopted in an operational forecasting service without significantly affecting the service's timeliness.

2.5. Verification procedure

Precipitation data collected from a network of more than 200 rain gauges, operated by NOA and spread across the Greek territory (Fig. 2b) were used for evaluating the performance of the implemented lightning data assimilation technique. Since the key objective of the present study is to examine the capacity of the data assimilation technique with regards to improving precipitation forecasting, the verification procedure focused primarily on the forecast period of each numerical simulation. For this, the 24 h accumulated precipitation (T0 + 6 to T0+30, where T0 is the

Table 1
Summary of the synoptic-scale setup of the eight precipitation events.

Case	Group	Main characteristics
20–21 May 2010	NWS[b], ILA[c]	Low of ~1011 hPa west of Italy (20 May 2010), moving eastwards (~1009 hPa west of Greece, 21 May 2010). 24 h accumulated precipitation[a] exceeded 50 mm in three stations (2 in north Greece, 1 in west Greece). Significant lightning over west and central Greece during the assimilation period.
18–19 February 2011	WS[d], SLA[e]	Low of ~997 hPa over the Gulf of Sidra (18 February 2011), moving north-eastwards (~995 hPa southwest of Greece, 19 February 2011). 24 h accumulated precipitation exceeded 70 mm in three stations in north Greece. Significant lightning over southwest Greece during the assimilation period.
14–15 May 2012	NWS, ILA	Low of ~1009 hPa over Albania (14 May 2012), moving southwards (~1002 hPa over central Aegean Sea, 15 May 2012). 24 h accumulated precipitation exceeded 35 mm in four stations in north Greece. Significant lightning over northwest and north–central Greece during the assimilation period.
29–30 December 2012	WS, SLA	Low of ~1010 hPa in west Greece (29 December 2012), moving south-eastwards (~1009 hPa over Crete island, 30 December 2012). 24 h accumulated precipitation exceeded 100 mm in six stations in south Greece. Significant lightning over central-south Aegean Sea during the assimilation period.
07–08 February 2013	NWS, SLA	Low of ~995 hPa in northern Balkans (07 February 2013), moving rapidly southwards (~996 hPa over north Greece, 08 February 2013). 24 h accumulated precipitation exceeded 40 mm in two island stations in south-east Aegean Sea. Significant lightning activity across the Aegean Sea during the assimilation period.
13–14 February 2013	NWS, SLA	Low of ~1001 hPa in south Italy (13 February 2013), moving south-eastwards (~1009 hPa over southwest Greece, 14 February 2013). 24 h accumulated precipitation exceeded 40 mm in three island stations in south Aegean Sea. Significant lightning over northwest Greece and across central–north Aegean Sea.
30 September-01 October 2013	WS, ILA	Successive short-wave troughs moving eastwards over Greece. 24 h accumulated precipitation exceeded 60 mm in five stations in south Greece. Significant lightning over west Greece during the assimilation period.
13–14 November 2013	WS, ILA	Almost stationary low of ~1009 hPa in south Italy. 24 h accumulated precipitation exceeded 50 mm in three stations in central Greece. Significant lightning over southwest Ionian Sea during the assimilation period.

[a] The 24 h accumulated precipitation refers to the period from 1800Z of the first day of the event through 1800Z of the second day.
[b] NWS: Non-widespread precipitation events.
[c] ILA: Intense lightning activity events.
[d] WS: Widespread precipitation events.
[e] SLA: Scarce lightning activity events.

model's initialization time) at the innermost modeling domain (DO2; Fig. 2a) was verified against observed data from the rain gauge network of NOA (Fig. 2b). For the verification, the nine model grid points surrounding each rain gauge were first considered. The grid point with the closest value to the observed was consequently chosen to represent the predicted value. This approach was adopted to avoid penalizing model performance due to small displacements of precipitation, which may result from the specified horizontal resolution.

The verification of model performance under the different numerical experiments was primarily based on a categorical dichotomous statement (i.e. yes/no statement) for five distinct precipitation thresholds: above 1 mm, 2.5 mm, 5 mm, 10 mm and 20 mm. Given the matched pairs of precipitation predictions and observations, a 2 × 2 contingency table was built for each threshold. The scores consequently computed in this study include: (a) the probability of detection (POD), the false alarm ratio (FAR), and (c) the critical success index (CSI) or threat score.

The above reported statistical measures do not account for the magnitude of precipitation errors. As such, they cannot be strictly used for estimating the error of precipitation predictions. For this, the mean absolute error (MAE) was computed. Similarly to the qualitative verification scores, calculation of MAE was carried out for five precipitation ranges, defined based on observed data: [0.1, 2.5 mm), [2.5, 5 mm), [5, 10 mm), [10, 20 mm), ≥20 mm.

In addition to the statistical verification, one event is selected and presented in more details. This approach was followed to allow for investigating the impact of lightning forcing on the simulated rainfall distribution, in association with modifications induced on the mesoscale environment.

2.5.1. Determination of statistical significance

When carrying out comparisons of model performance under different configurations, it is important that a measure of uncertainty in score differences be defined. Considering the qualitative statistical measures (i.e. POD, FAR and CSI), this can be achieved by conducting a hypothesis test to verify that a score difference between two competing “models” is statistically significant at a pre-defined confidence interval. In this study, the hypothesis test approach implemented is the one originally proposed by Hamill (1999), as adapted by Accadia et al. (2003, 2005). This approach is based on the construction of a probability density function (PDF) that is consistent with the selected null hypothesis. A brief description of the method is provided herein; a comprehensive description and discussion of the method is available in Hamill (1999) and Accadia et al. (2003).

The null hypotheses (H_0) adopted in the present study are that the differences in the verification scores (SCR) between the CNTL and either the LTNGDA or LTNGDA_NS model experiments are zero:

$$H_0 : SCR_i - SCR_{CNTL} = 0.0 \quad (1)$$

The alternative hypotheses are:

$$H_1 : SCR_i - SCR_{CNTL} \neq 0.0 \quad (2)$$

In Eqs. (1) and (2), SCR is one of the computed scores (i.e. POD, FAR, or CSI) and i an index corresponding to either the LTNGDA or the LTNGDA_NS experiment. The verification scores were computed for each threshold after summing the contingency tables that were constructed for each of the eight examined cases. This process effectively allows for minimizing the sensitivity of the scores to small changes in the elements of contingency tables (Hamill, 1999).

Random sampling of the contingency tables was carried out 100,000 times for each comparison (i.e. CNTL versus either LTNGDA or LTNGDA_NS) at each threshold, using the bootstrap method (Diaconis and Efron, 1983), as presented in Accadia et al. (2003, 2005). Through this approach, the PDF of score differences consistent with the null hypothesis (Eq. (1)) was first built. The hypothesis of difference in the verification scores was consequently tested by specifying the location of the actual score differences in the distribution of the resampled differences (Hamill, 1999). The significance test was performed assuming a 90% ($\alpha = 0.10$) and a 95% ($\alpha = 0.05$) confidence interval.

The statistical significance of the differences in MAE between the conducted experiments was also evaluated. Since this particular statistical measure is directly derived from observed and modelled data, the non-parametric Wilcoxon signed-rank test (Wilks, 1995) was used, assuming a 90% and 95% confidence interval. According to Hamill (1999), this statistical test is considered to be a good alternative to the resampling technique implemented for the scores derived from contingency tables.

3. Results and discussion

To assess the overall performance of the lightning data assimilation technique, verification scores (Sec. 2.5) for the 24 h accumulated precipitation were first examined over all cases. At a second stage, the studied events were split into two groups and verification measures were then examined over the events of each group. The criterion used for grouping the events was the occurrence of 24 h accumulated precipitation exceeding 20 mm at more than 25% of the considered rain gauges. The events that met this criterion were classified into the "widespread" (WS) precipitation group, whereas the rest of the events were grouped to form the "non-widespread" (NWS) precipitation group (Table 1). In essence, this categorization allows for examining the performance of the lightning data assimilation technique during the occurrence of spatially more extensive (i.e. WS) or more restricted (i.e. NWS) high precipitation events. One could argue on this, supposing that for the NWS events the number of gauges reporting >20 mm precipitation is small, thus not allowing for a sound verification at the above threshold. However, it should be underlined that all NWS events exhibit a satisfactory number of >20 mm measurements, ensuring the quality of the computed statistics.

Last, the considered events were categorized depending on the total number of WRF grid points affected during the assimilation period. In particular, all events with >1000 model grid boxes exhibiting at least 1 lightning count were classified into the "intense lightning activity" (ILA) group, whereas the rest of the events were categorized into the "scarce lightning activity" (SLA) group (Table 1). Such a classification allows for examining any possible dependence of the assimilation scheme on the amount of observed data employed for assimilation in WRF.

3.1. 24 h accumulated precipitation

Overall, an improvement can be seen in the statistical scores when lightning data are ingested in the model (Fig. 3). More importantly, the positive impact on precipitation prediction is found to be statistically significant (at least at $\alpha = 0.10$) and most profound for the highest rain threshold (i.e. >20 mm). This confirms earlier similar studies reporting on the stronger potential of lightning data assimilation in areas of high precipitation amounts (Papadopoulos et al., 2005, 2009; Lagouvardos et al., 2013) rather than in regions with low to moderate precipitation accumulations. Considering that lightning activity is directly related to the occurrence of vigorous convection, the expectation for improving prediction of intense precipitation appears to be quite successfully met.

The impact of lightning data assimilation on the prediction of intense precipitation is found to be generally greater for the LTNGDA_NS experiment than for the LTNGDA. This is primarily highlighted by the large reduction seen in FAR (Fig. 3b), equaling 25%, as well as by the statistically significant improvement of CSI that approximates 10% (Fig 3c). On the other hand, LTNGDA shows a large relative increase in FAR for the moderate threshold of >10 mm (Fig. 3b). This unwanted effect could be associated with the activated option to suppress the KF scheme in the absence of observed lightning. Using the same lightning data assimilation technique in the COAMPS model, Mansell et al. (2007) also reported less spurious precipitation in their numerical simulations when convection was not actively prevented from being initiated (i.e. LTNGDA_NS in this study). This can be attributed to the fact that the considered CPS may be naturally suppressed by the compensating subsidence originating from past convection, since some positive vertical motion is required to activate the trigger function (Fritsch and Chappell, 1981).

3.2. WS and NWS events

Examining separately WS and NWS events, it is evident that even without the assimilation of lightning, WRF performs better when intense precipitation (>20 mm) occurs extensively across the study area (Fig. 4) than when it occurs more locally (Fig. 5). However, this is not a very surprising differentiation in the model's performance. For instance, Liu et al. (2012) recently reported that WRF shows the best performance in reproducing precipitation events characterized by spatiotemporal evenness of the observed rainfall, as is generally the case of the WS events in the present study.

The ingestion of lightning data appears to further improve model performance, especially considering the WS events. For the highest rain threshold, LTNGDA_NS is found to induce relative improvements of 9%, 27% and 12% (statistically significant at least at $\alpha = 0.10$) in POD (Fig. 4a), FAR (Fig. 4b) and CSI (Fig. 4c), respectively, as well as a reduction in the predictions' MAE by 5% (Fig. 4d; statistically significant at $\alpha = 0.05$). LTNGDA also results to overall improved precipitation predictions of intense rain, but its impact is found to be lower than in the case of LTNGDA_NS. The large increase seen in FAR (statistically significant at $\alpha = 0.10$) when LTNGDA is examined could be due to the implemented approach of suppressing the KF scheme when no lightning is observed, an effect that has been previously discussed.

Examining NWS events (Fig. 5), lower overall improvements are found for both LTNGDA and LTNGDA_NS experiments. The differences in the impact of the two assimilation experiments on model performance are found to be small, while this impact is only found to be statistically significant ($\alpha = 0.10$) for low and moderate rain thresholds. This is true for all verification scores (Fig. 5a–c) except for MAE (Fig. 5d) where a statistically significant reduction of 5% was computed for the highest rain threshold when LTNGDA was examined. This rather restricted enhancement of model performance, as compared to the results obtained for the WS events, could be attributed, at least partially, to the inherit difficulty, previously discussed, of the WRF model to reproduce spatially uneven precipitation events (Liu et al., 2012), as is generally the case of NWS events considered in this study. Even with the forced initiation of convection through the ingestion of lightning, it appears that it is difficult for the model to reproduce precipitation events that occur more locally rather than those affecting larger areas. This is an interesting finding that deserves to get more attention in future applications of the assimilation technique, especially considering that similar studies have been, most frequently, focusing on extensive and generally extreme events.

3.3. ILA and SLA events

Results indicate that the impact of lightning assimilation on model performance is not significantly influenced by the amount of data being ingested. Indeed, for both ILA (Table 2) and SLA (Table 3) events precipitation prediction is overall improved. This enhances the reliability and robustness of the assimilation scheme, which proves itself capable of positively influencing model performance

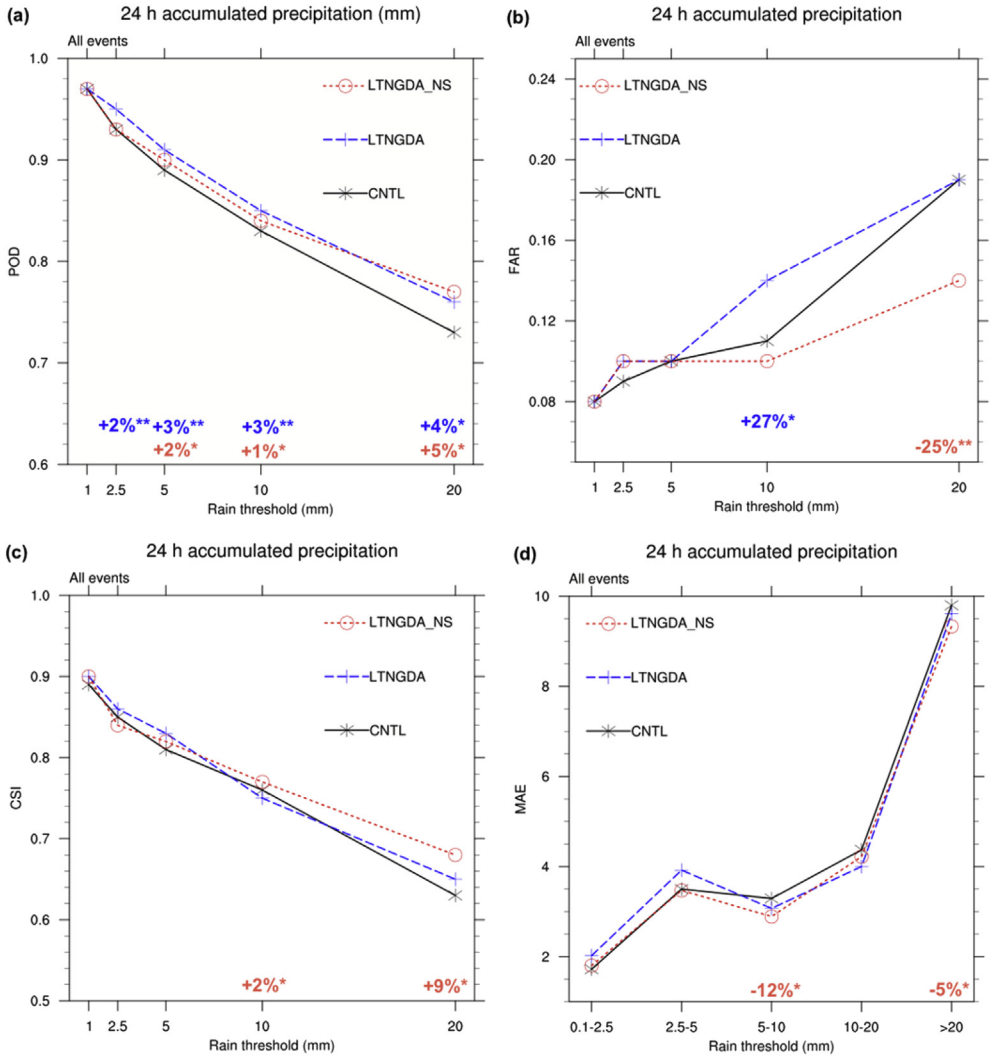

Fig. 3. Verification scores for various 24 h accumulated precipitation thresholds of the different numerical experiments conducted with the WRF model, considering all 8 cases: (a) probability of detection, (b) false alarm ratio, (c) critical success index, and (d) mean absolute error. Percentages above a precipitation threshold indicate statistically significant (one asterisk denotes $\alpha = 0.10$, two asterisks denote $\alpha = 0.05$) relative changes in scores. The different font colour used for the percentages corresponds to the colour assigned to each of the two assimilation experiments (i.e. blue: LTNGDA, red: LTNGDA_NS). (For interpretation of the references to colour in this figure legend, the reader is referred to the web version of this article.)

under both restricted and abundant lightning data availability during the assimilation period.

Similarly to what has been previously presented and discussed, LTNGDA_NS is found to be more consistent than LTNGDA in improving overall model performance (Tables 2 and 3). This is particularly true for the highest rain threshold (>20 mm), for which statistically significant (at least at $\alpha = 0.10$) improvements in all verification scores can be seen when LTNGDA_NS is considered. On the other hand, the major deficiency of LTNGDA appears to be the reduced ability to restrict spurious precipitation (Mansell et al., 2007), an effect that has been previously discussed and that can lead to increased FAR scores as seen in Tables 2 and 3

Although the differences in the verification results between ILA (Table 2) and SLA (Table 3) events are generally small, one could notice that slightly larger improvements are found when intense lightning activity takes place during the assimilation period (i.e. ILA events). This is more evident focusing on LTNGDA_NS and especially examining MAE, a quantitative statistical measure. In particular, a considerably large (~20%) and statistically significant ($\alpha = 0.05$) reduction can be seen in MAE for the highest rain threshold under the LTNGDA_NS experiment for the ILA events (Table 2). Conversely, for the SLA events MAE values are found to be larger than for ILA events and reductions induced by either LTNGDA or LTNGDA_NS can be seen to be smaller and statistically significant only at lower rain thresholds.

4. Example case study: 13–14 November 2013

The selected event, starting on 13 November 2013, is considered to be a typical example of weather systems that frequently affect the study area, resulting in heavy precipitation and, occasionally, flash floods. At 1200Z 13 November a cut-off low at 500 hPa is present south of Italy (Fig. 6a). In the next 12 h (0000Z 14 November) the upper-level system begins to weaken, moving slowly north-eastwards (Fig. 6b) and gradually giving place to the development of a weak upper-air short-wave trough (Fig. 6c). This particular synoptic setup indicates that during the examined event, unstable atmospheric conditions dominated the study area, resulting in strong ascending motions and convective activity.

Observed and simulated precipitation accumulations over the

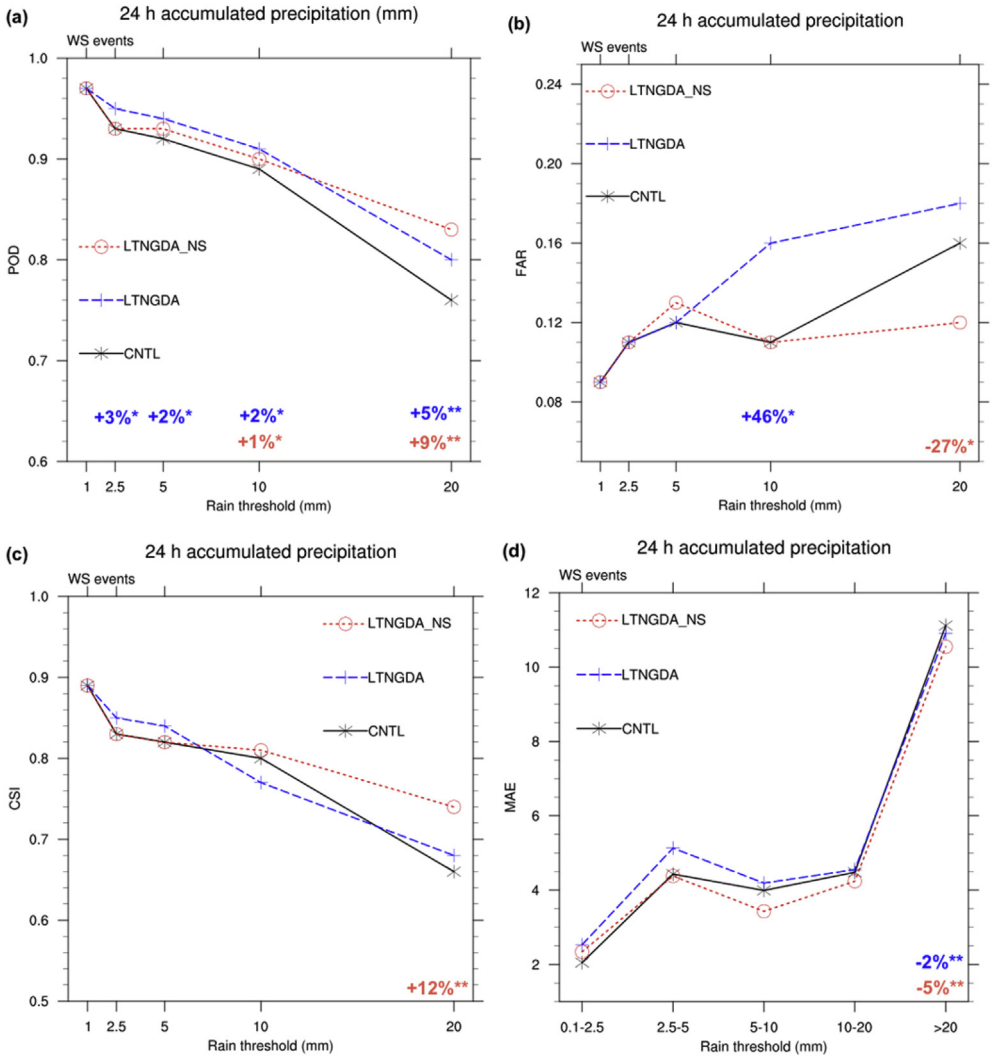

Fig. 4. Same as Fig. 3 but with verification scores averaged over the 4 WS events.

first two 6 h forecast periods are presented in Fig. 7 (13 November 1800Z to 14 November 0000Z) and Fig. 9 (14 November 0000Z to 14 November 0600Z). The decision to only focus on the first 12 h of the forecast period has been made for the sake of clarity, taking also into consideration that the heaviest rainfall amounts were recorded in this time window of the examined event.

Significant differences can be seen in the first 6 h forecast period (13 November 2013 1800Z to 14 November 2013 0000Z), between the modeled and observed rainfall distribution when lightning data are not assimilated. For instance, the south-to-north oriented band of heavy rain simulated in CNTL experiment (Fig. 7b) over Peloponnesus, is a feature not supported by observations (Fig. 7a). In addition, precipitation is significantly overestimated over the islands of Kefalonia and Zakynthos. When lightning data are assimilated, one can easily notice that precipitation simulation generally improves. Evidently, the most striking feature common to both assimilation experiments (Fig. 7c, d) is the more realistic representation of rainfall over Peloponnesus. This is primarily highlighted by the removal of the erroneous heavy rain band and the more accurate reproduction of rainfall in north/central Peloponnesus and in the vicinity of the Myrtoan Sea, where the highest accumulations were actually observed (Fig. 7a). On the other hand, LTNGDA and LTNGDA_NS also exhibit differences that are particularly significant over Kefalonia and Zakynthos. Clearly, the experiment that employed active suppression of the KF CPS (Fig. 7c) improved precipitation prediction over both islands, contrary to the experiment that did not actively suppress convection (Fig. 7d), which enhanced the unrealistically high rainfall amounts present in the CNTL experiment (Fig. 7b).

The above reported difference between LTNGDA and LTNGDA_NS is also reflected on the 10 m wind field and 850 hPa equivalent potential temperature (θ_e), 1 h following the end of the assimilation period (13 November 2013 1900Z). As seen in Fig. 8, both assimilation experiments indicate the formation of a cold pool in north-west Peloponnesus, a feature that is not present in the CNTL experiment. However, LTNGDA results' (Fig. 8b) suggest a stronger and wider cold pool than the one reproduced by LTNGDA_NS (Fig. 8c). Apparently, the active suppression of the model's CPS allowed for increased grid-scale precipitation in the examined area (not shown), thus strengthening evaporative cooling. The different intensity and coverage of this particular cold pool, along with its associated outflow boundary, seem to be the reason for the differences in precipitation, between the two assimilation experiments, over the islands of Kefalonia and Zakynthos.

Examination of the closest in time operational analysis, derived from the European Centre for Medium-Range Weather Forecasts

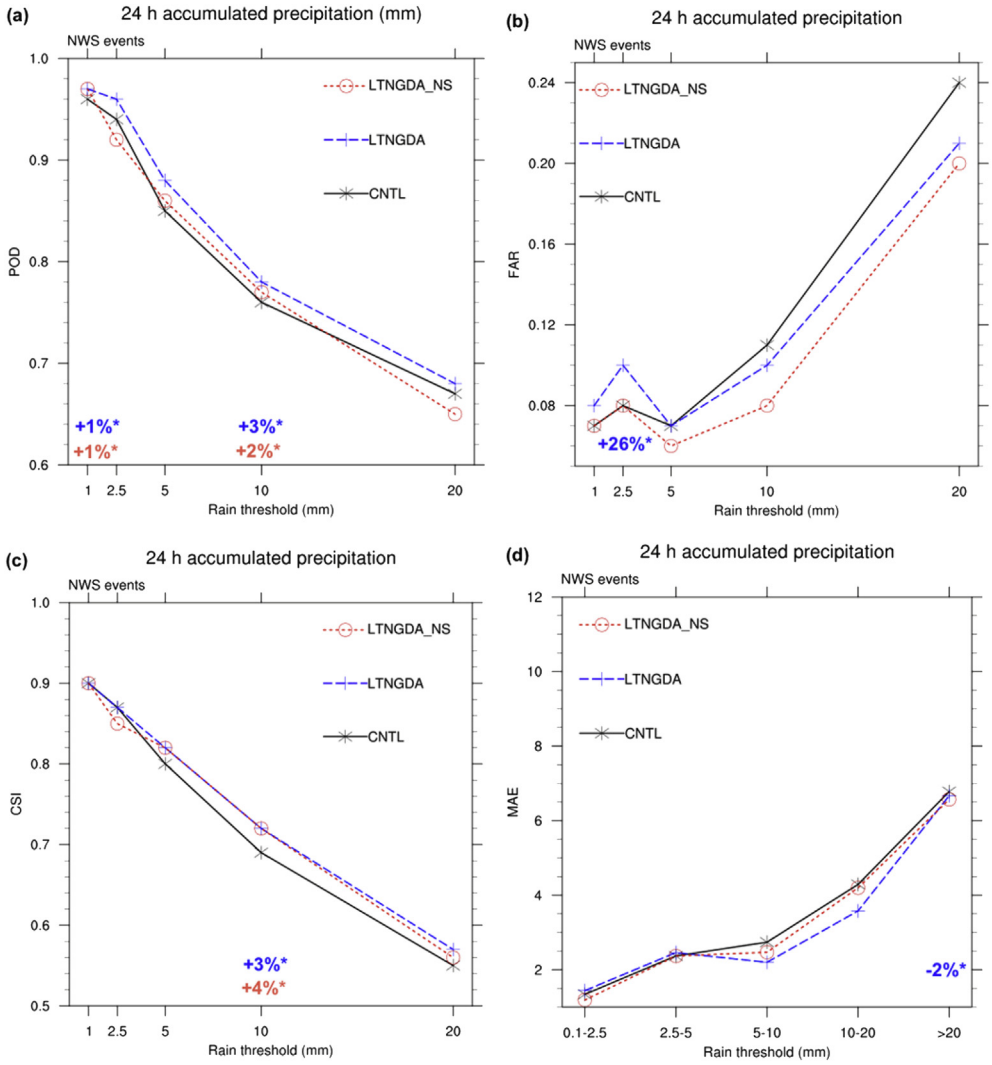

Fig. 5. Same as Fig. 3 but with verification scores averaged over the 4 NWS events.

Table 2
Summary of verification scores for various 24 h accumulated precipitation thresholds of the different numerical experiments conducted with the WRF model, considering ILA events. Statistically significant changes are highlighted in bold (one asterisk denotes $\alpha = 0.10$, two asterisks denote $\alpha = 0.05$).

	POD				
	>1 mm	>2.5 mm	>5 mm	>10 mm	>20 mm
CNTL	0.96	0.93	0.91	0.86	0.73
LTNGDA	0.97*	0.95*	0.93	0.89*	0.75
LTNGDA_NS	0.97	0.92	0.91	0.88*	0.77*
	FAR				
	>1 mm	>2.5 mm	>5 mm	>10 mm	>20 mm
CNTL	0.08	0.10	0.09	0.11	0.19
LTNGDA	0.08	0.09	0.09	0.14	0.20
LTNGDA_NS	0.08	0.10	0.11	0.10	0.14*
	CSI				
	>1 mm	>2.5 mm	>5 mm	>10 mm	>20 mm
CNTL	0.89	0.84	0.84	0.78	0.62
LTNGDA	0.90	0.87	0.85	0.78	0.63
LTNGDA_NS	0.89	0.84	0.82	0.80*	0.69*
	MAE				
	[0.1, 2.5 mm)	[2.5, 5 mm)	[5, 10 mm)	[10, 20 mm)	≥20 mm
CNTL	1.97	2.23	3.90	4.38	6.90
LTNGDA	2.27	2.17	3.51	4.00	7.00
LTNGDA_NS	2.36	2.11	3.12	4.00	5.86**

Table 3
Same as Table 2 but with verification scores referring to SLA events.

	POD				
	>1 mm	>2.5 mm	>5 mm	>10 mm	>20 mm
CNTL	0.97	0.94	0.86	0.79	0.73
LTNGDA	0.97	0.96	0.90*	0.81*	0.78*
LTNGDA_NS	0.97	0.93	0.89*	0.80	0.77*
	FAR				
	>1 mm	>2.5 mm	>5 mm	>10 mm	>20 mm
CNTL	0.07	0.09	0.11	0.10	0.18
LTNGDA	0.08	0.12*	0.11	0.13*	0.18
LTNGDA_NS	0.07	0.10	0.09*	0.09	0.14*
	CSI				
	>1 mm	>2.5 mm	>5 mm	>10 mm	>20 mm
CNTL	0.90	0.86	0.78	0.73	0.63
LTNGDA	0.90	0.85	0.81	0.72	0.66
LTNGDA_NS	0.90	0.85	0.82*	0.74	0.68*
	MAE				
	[0.1, 2.5 mm)	[2.5, 5 mm)	[5, 10 mm)	[10, 20 mm)	≥20 mm
CNTL	1.54	4.69	2.80	4.37	13.13
LTNGDA	1.84	5.56	2.72**	3.99	12.62
LTNGDA_NS	1.40*	4.75	2.70	4.46	13.34

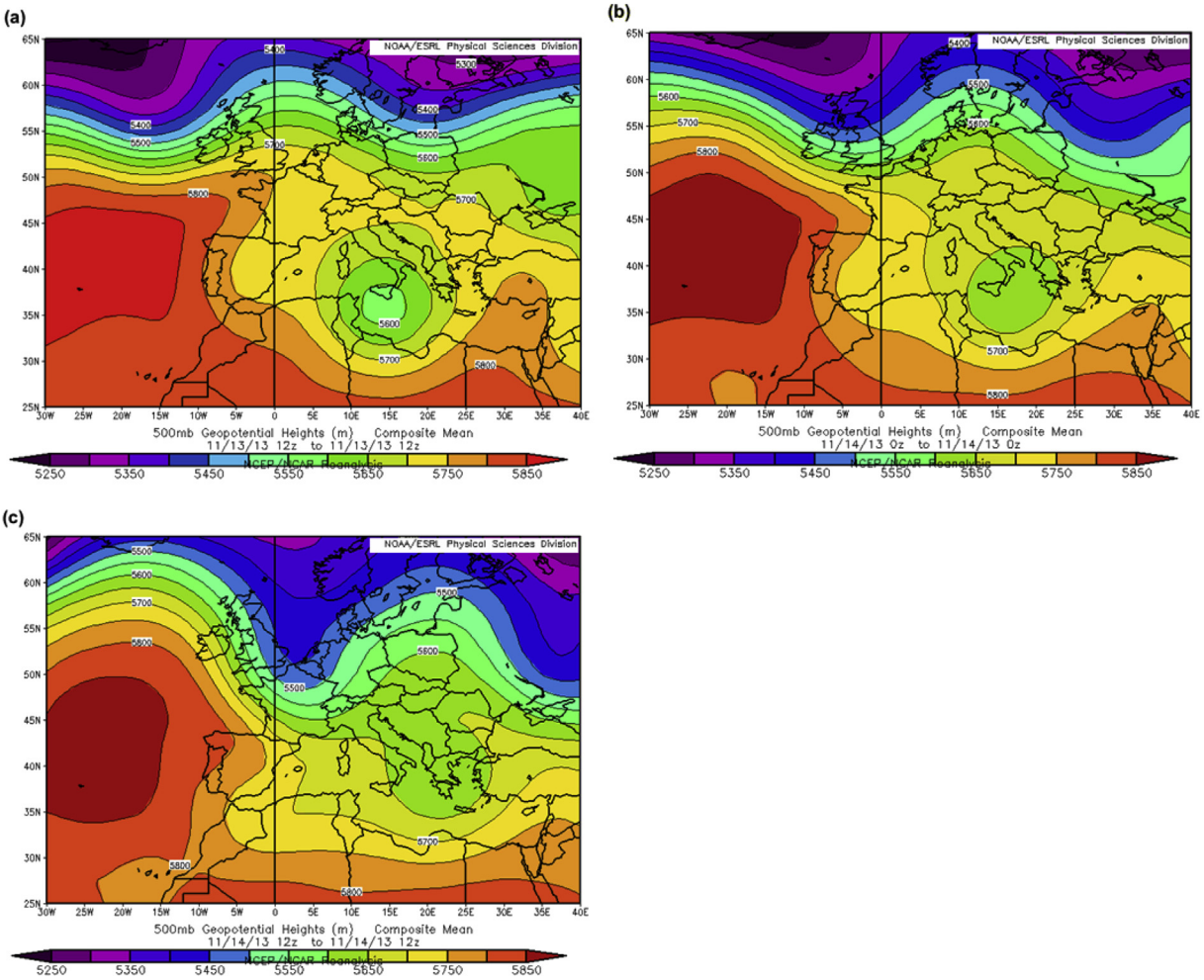

Fig. 6. 500 hPa geopotential heights (at 50 gpm intervals) derived from NCEP/NCAR reanalyses (Kalnay et al., 1996), valid at (a) 1200Z 13 November 2013, (b) 0000Z 14 November 2013, and (c) 1200Z 14 November 2013 (Images provided by the NOAA/ESRL Physical Sciences Division, Boulder Colorado from their website at http://www.esrl.noaa.gov/psd/).

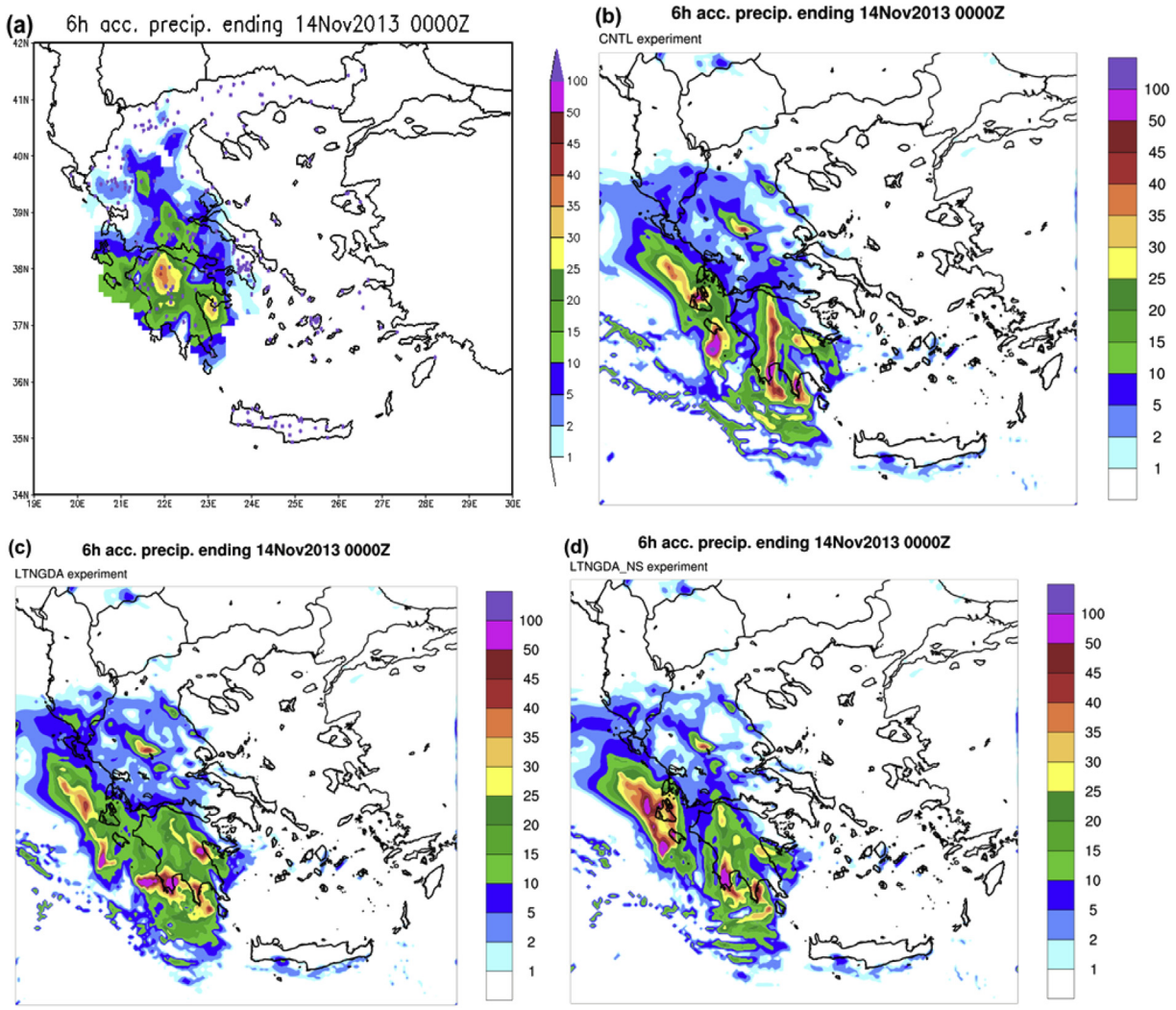

Fig. 7. Observed and simulated 6 h accumulated precipitation ending at 14 November 2013 0000Z: (a) Rain gauge data, (b) CNTL WRF experiment, (c) LTNGDA WRF experiment, and (d) LTNGDA_NS WRF experiment.

(ECMWF) at a 0.125°× 0.125 horizontal resolution, confirms that the assimilation of lightning does improve the representation of the mesoscale environment. For instance, Fig. 8d indicates that the advection of warm unstable air (higher θ_e values) is confined to the area south-west of Peloponnesus, whereas colder and more stable air (lower θ_e values) is present over north-west Peloponnesus, in the vicinity of Kefalonia and Zakynthos islands. This particular mesoscale setup seems to be better resolved in LTNDGA (Fig. 8b) and LTNGDA_NS experiments (Fig. 8c) than in the CNTL simulation (Fig. 8a).

Examination of the second 6 h forecast period (14 November 2013 0000Z to 14 November 2013 0600Z) reveals that WRF is capable of maintaining the information provided by the lightning data assimilation scheme during the 6 h initialization period (13 November 2013 1200Z to 13 November 2013 1800Z). In both assimilation experiments (Fig. 9c, d) precipitation is reduced in central Continental Greece, while in the wider region of the Myrtoan Sea and Cyclades, precipitation is increased. Compared to the CNTL experiment (Fig. 9b), the above changes result to a rainfall distribution that is, overall, in better agreement with observations (Fig. 9a). Similarly to what has been discussed for the first 6 h forecast period, the prevention of the KF scheme from activation in the absence of observed lightning seems to result to more realistic precipitation amounts. For instance, the overestimation of rainfall in central Continental Greece is lower for LTNGDA than LTNGDA_NS, while LTNGDA also manages to reproduce the observed maximum in south-west Attica. On the other hand, LTNGDA results' indicate an erroneous precipitation maximum over central Evia, not present in the case of LTNGDA_NS.

The effect of lightning forcing on the low-level atmospheric environment remains evident 7 h following the end of the assimilation period (14 November 2013 0100Z), as shown in Fig. 10. Compared to the experiment with no lightning data assimilation, both assimilation experiments are found to produce a stronger cold pool in the wider region of north Peloponnesus and central-south Continental Greece, a feature that is possibly linked to the previously reported decrease in the simulated precipitation in this area. Further, it seems that the ingestion of lightning enhances the advection of unstable warm and moist air (high θ_e values) in the Cyclades area, consequently increasing precipitation during the second 6 h forecast period.

Similarly to the previous 6 h forecast period, inspection of the corresponding ECMWF analysis (Fig. 10d) reveals an overall better representation of the mesoscale environment when lightning data are ingested in the model. This is particularly evident focusing on the areas of Peloponnesus and the Ionian Sea, for which the CNTL

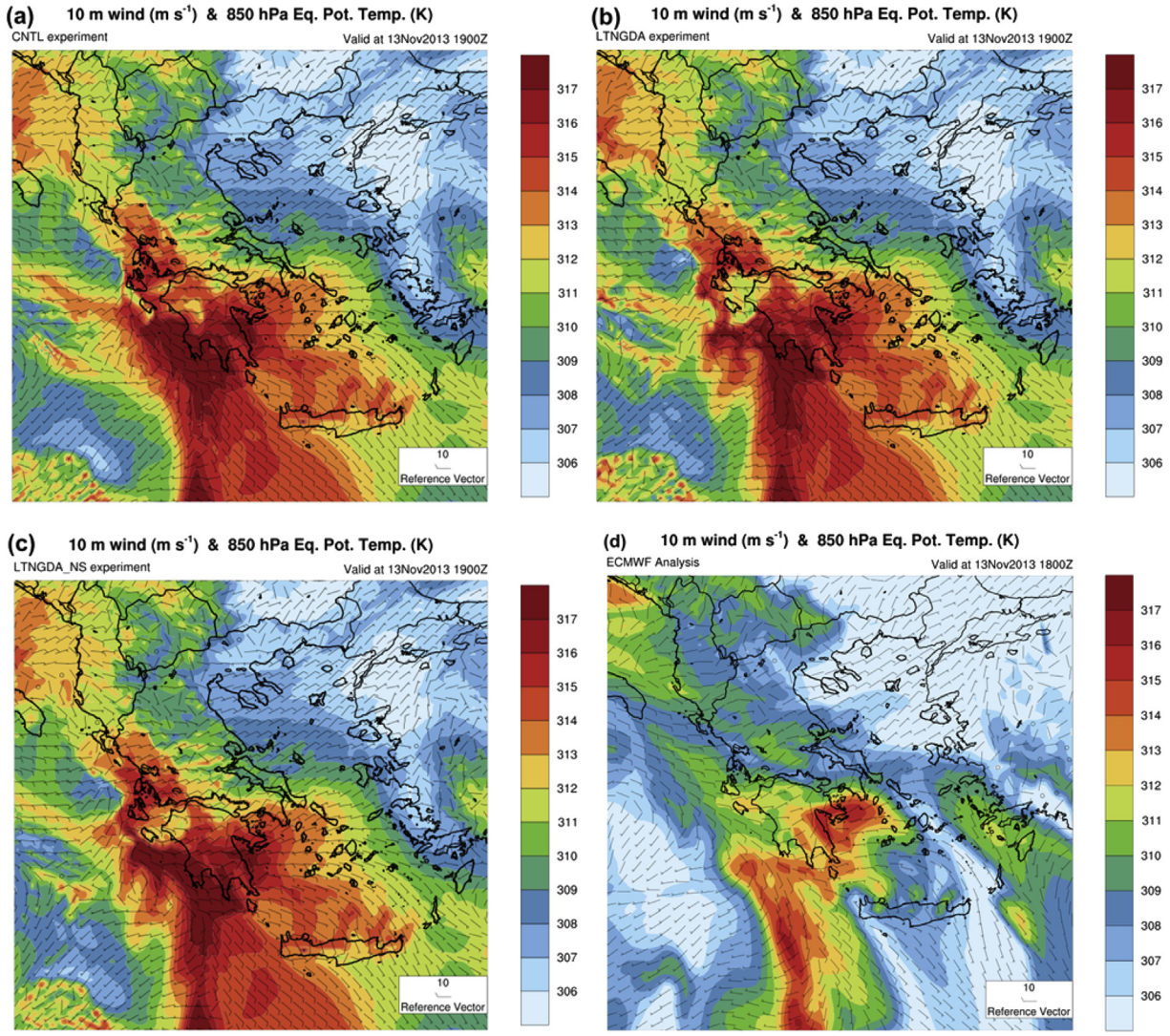

Fig. 8. 10 m wind barbs overlaid with 850 hPa equivalent potential temperature at 13 November 2013 from (a) CNTL WRF experiment, (b) LTNGDA WRF experiment, (c) LTNGDA_NS WRF experiment at 1900Z, and (d) ECMWF analysis at 1800Z. Note that the horizontal grid spacing for the WRF maps equals 6 km, while for the ECMWF map it approximates 12.5 km.

experiment (Fig. 10a) indicates the presence of unstable warm air (higher θ_e values). On the other hand, both LTNGDA (Fig. 10b) and LTNGDA_NS (Fig. 10c) experiments provide a representation closer to the analysis (Fig. 10d), characterized by colder and more stable air (lower θ_e values) over much of Peloponnesus and relatively warmer and less stable air (higher θ_e values) over the wider area of Kefalonia and Zakynthos islands.

Coming to the end of the discussion of this particular event, it should be underlined that limited data availability might restrict the conclusions drawn. For instance, large precipitation amounts simulated by either of the two assimilation experiments over the Ionian Sea and the west and central peninsulas of Peloponnesus (e.g. Fig. 7c, d) cannot be verified due to the spatial coverage of the measurement sites (Fig. 2b). Alternative data sources, such as radar imagery and/or radiosondes, which could be employed for strengthening the discussion of the present study's findings, were unfortunately not available.

5. Conclusions

A technique employing lightning data for improving precipitation prediction has been implemented in the WRF model. This technique (WRF-LTNGDA) utilizes lightning as a proxy for identifying the location of convective activity and, consequently, controlling the trigger function of the model's CPS. Although this cannot be considered to be a novel approach, it is still the first time that such an assimilation technique is incorporated in a widely implemented NWP model with the aim to evaluate its capacity for operational weather forecasting applications. In this context, the implemented lightning data assimilation technique has been evaluated over eight precipitation events that took place in Greece in the period 2010–2013. A short (i.e. 6 h) assimilation period, allowing for operational readiness, was adopted, and the consequent 24 h accumulated precipitation was verified against observations. Within this frame, this study deviates from similar past ones focusing on a single or a couple of extreme precipitation events.

The results of the present study clearly suggest that lightning forcing has a positive impact on precipitation prediction. Despite the restricted assimilation period, the ability of the model to correctly predict the occurrence/no occurrence of precipitation up to the next 24 h was found to improve. More importantly, the

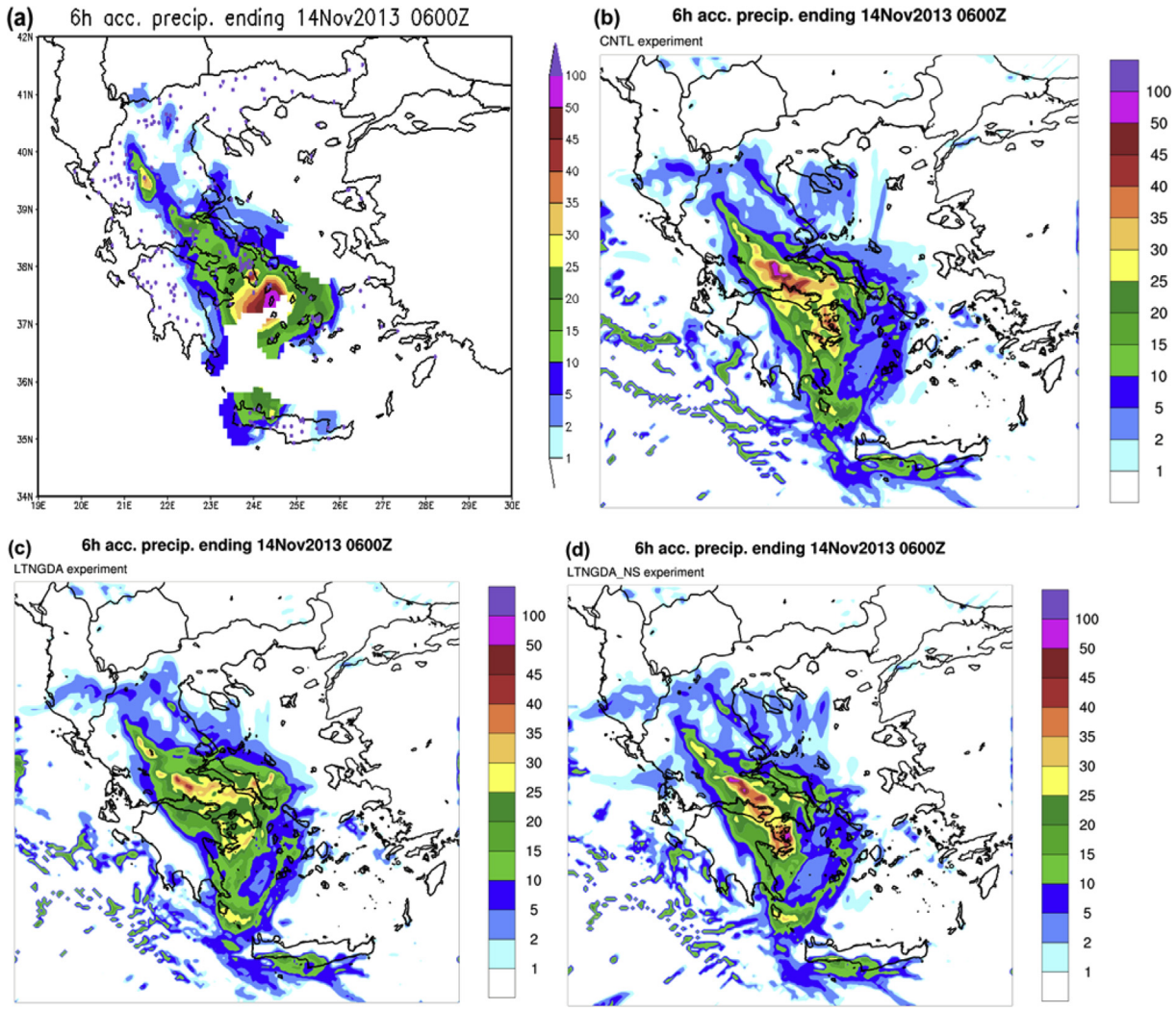

Fig. 9. Same as Fig. 7 but with 6 h accumulated precipitation ending at 14 November 2013 0600Z.

improvements induced on the computed verification scores were found to be statistically significant (at least at $\alpha = 0.10$), particularly for the intense precipitation thresholds. Examination of model performance for different groups of events revealed that the positive impact of lightning assimilation is generally larger for cases with extensive occurrence of intense precipitation, rather than for cases with more local intense rainfall occurrence. The conducted analysis also revealed no significant dependence of the performance of assimilation on the amount of data used during the assimilation period.

In the current implementation of the lightning data assimilation technique, the model's CPS may or may not be prevented from generating convection when lightning is not observed. The adoption of one or the other option consequently modifies the impact of lightning assimilation on model performance. Overall, and in agreement with the original work of Mansell et al. (2007), it was found that active suppression of the CPS might occasionally increase spurious precipitation. However, this effect was found to be primarily evident in moderate rainfall amounts, being almost absent for intense accumulations.

Closer inspection of model performance under the different numerical experiments was carried out focusing on a single precipitation event. The results of this analysis highlighted an overall better subjective agreement between the simulated and observed rainfall distributions when lightning forcing was applied. In both experiments employing lightning data assimilation, WRF was found to be able to better reproduce precipitation distribution, removing erroneous intense rainfall bands and more correctly placing rainfall maxima. Differences between the two assimilation experiments did exist, mostly attributed to the different modification of the low-level atmospheric environment.

The present study demonstrates that the lightning data assimilation technique proposed by Mansell et al. (2007), as adapted by Lagouvardos et al. (2013), is sufficiently capable of improving precipitation prediction, particularly in the context of operational weather forecasting activities. This is primarily highlighted by the restrictions that were applied for the evaluation of the technique. First, a very short assimilation period, equaling 6 h, was set in order to account for the necessity for operational readiness of the modeling system. Second, the employed data were restricted to CG lightning, which represents only a small part of the total lightning activity. Given the above two significant restrictions, the statistically significant overall improvements seen in precipitation prediction become more important. Nevertheless, the evaluation of the presented lightning assimilation technique should be continued, focusing on longer forecast periods and possibly using alternative lightning data sources.

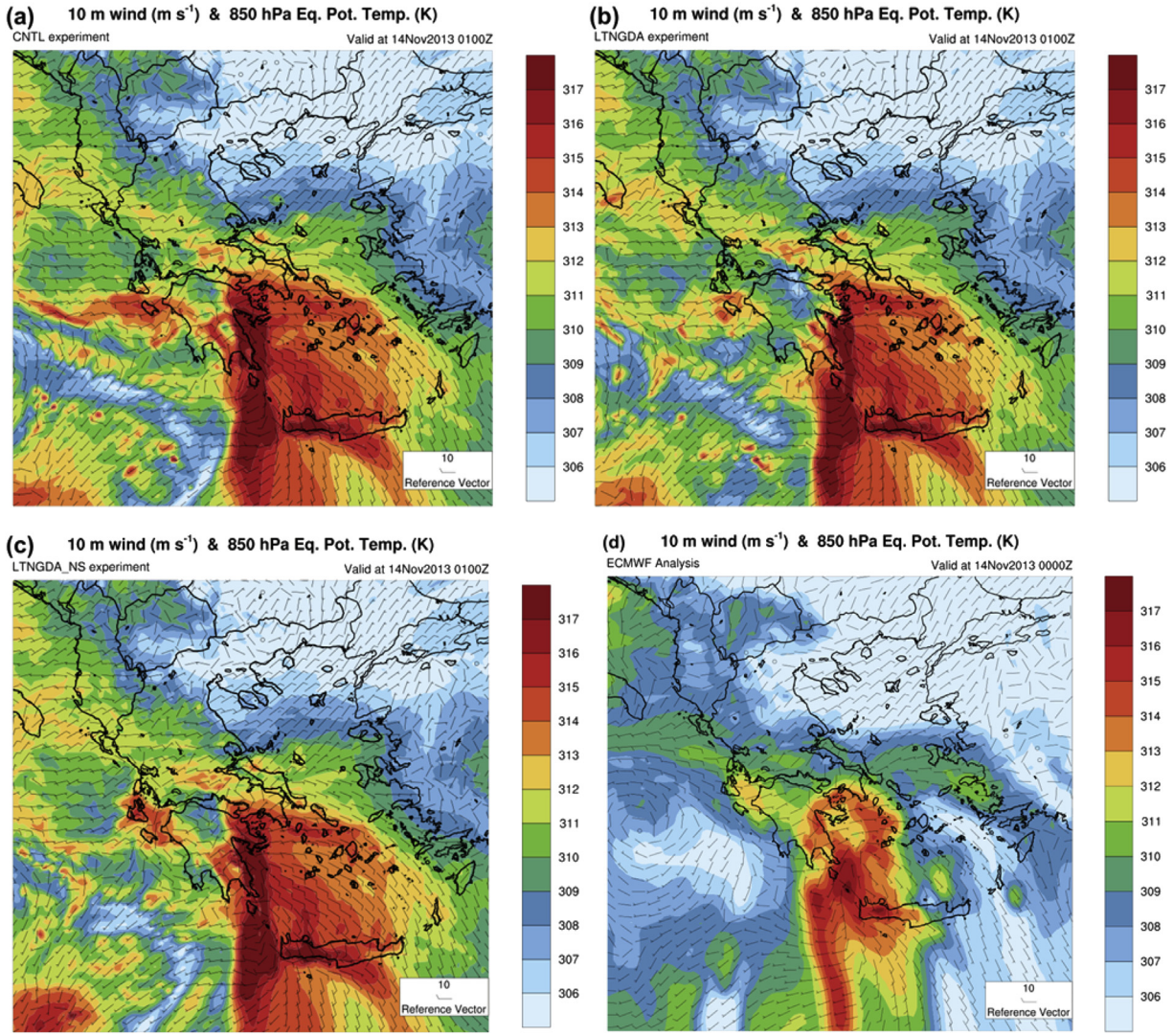

Fig. 10. Same as Fig. 9 but for 14 November 2013 0100Z (WRF) and 0000Z (ECMWF).

Acknowledgements

The authors acknowledge funding by the European Union (European Social Fund) and National Resources under the "ARISTEIA II" action of the Operational Programme "Education and Lifelong Learning" in Greece, Project TALOS-3449.

References

Accadia, C., Mariani, S., Casaioli, M., Lavagnini, A., 2003. Sensitivity of precipitation forecast skill scores to bilinear interpolation and a simple nearest-neighbor average method on high-resolution verification grids. Weather Forecast. 18, 918–932.

Accadia, C., Mariani, S., Casaioli, M., Lavagnini, A., Speranza, A., 2005. Verification of precipitation forecasts from two limited-area models over Italy and comparison with ECMWF forecasts using a resampling technique. Weather Forecast. 20, 276–300.

Alexander, G.D., Weinman, J.A., Karyampoudi, V.M., Olson, W.S., Lee, A.C.L., 1999. The effect of assimilating rain rates derived from satellites and lightning on forecasts of the 1993 superstorm. Mon. Weather Rev. 127, 1433–1457.

Carvalho, D., Rocha, A., Gomez-Gesteira, M., Santos, C., 2012. A sensitivity study of the WRF model in wind simulation for an area of high wind energy. Env. Mod. Softw. 33, 23–34.

Chang, D.E., Weinman, J.A., Morales, C.A., Olson, W.S., 2001. The effect of spaceborn microwave and ground-based continuous lightning measurements on forecasts of the 1998 Groundhog Day storm. Mon. Weather Rev. 129, 1809–1833.

Chen, F., Dudhia, J., 2001. Coupling an advanced land surface-hydrology model with the Penn State-NCAR MM5 modeling system. Part I: model implementation and sensitivity. Mon. Weather Rev. 129, 569–585.

Davidson, N.E., Puri, K., 1992. Tropical prediction using dynamical nudging, satellite-defined convective heat sources, and a cyclone bogus. Mon. Weather Rev. 120, 2501–2522.

Diaconis, P., Efron, B., 1983. Computer-intensive methods in statistics. Sci. Am. 248, 116–130.

Dudhia, J., 1989. Numerical study of convection observed during the winter monsoon experiment using a mesoscale two-dimensional model. J. Atmos. Sci. 46, 3077–3107.

Dudhia, J., 1993. A non-hydrostatic version of the Penn State/NCAR mesoscale model: validation tests and simulation of an Atlantic cyclone and cold front. Mon. Weather Rev. 121, 1493–1513.

Fierro, A.O., Mansell, E.R., Ziegler, C.L., MacGorman, R., 2012. Application of a lightning data assimilation technique in the WRF-ARW model at cloud-resolving scales for the tornado outbreak of 24 May 2011. Mon. Weather Rev. 140, 2609–2627.

Fierro, A.O., Gao, J., Ziegler, C.L., Mansell, R., MacGorman, D.R., Dember, S.R., 2014. Evaluation of a cloud-scale lightning data assimilation technique and a 3DVAR method for the analysis and short-term forecast of the 29 June 2012 derecho event. Mon. Weather Rev. 142, 183–202.

Fritsch, J.M., Chappell, C.F., 1981. Preliminary numerical tests of the modification of mesoscale convective systems. J. Appl. Meteor 20, 910–921.

Gauthier, M.L., Petersen, W.A., Carey, L.D., Christian Jr., H.J., 2006. Relationship between cloud-to-ground lightning and precipitation ice mass: a radar study over Houston. Geophys. Res. Lett. 33, L20803. http://dx.doi.org/10.1029/2006GL027244.

Goodman, S.J., Buechler, D.E., Wright, P.D., Rust, W.D., 1988. Lightning and precipitation history of a microburst-producing storm. Geophys. Res. Lett. 15,

1185–1188.
Hamill, T.M., 1999. Hypothesis tests for evaluating numerical precipitation forecasts. Weather Forecast. 14, 155–167.
Hodur, R.M., 1997. The naval research Laboratory's coupled Ocean/Atmosphere mesoscale prediction system (COAMPS). Mon. Weather. Rev. 125, 1414–1430.
Janjic, Z.I., 1994. The step-mountain eta coordinate model: further developments of the convection, viscous sublayer and turbulence closure schemes. Mon. Weather Rev. 122, 927–945.
Janjic, Z.I., 1996. The surface layer in the NCEP Eta model. In: Eleventh Conference on Numerical Weather Prediction, Norfolk, VA, 19–23 August, Amererican Meteor Society, Boston, MA, pp. 345–355.
Janjic, Z.I., 2002. Nonsingular Implementation of the Mellor-yamada 2.5 Scheme in the NCEP Meso Model, p. 61. NCEP Office Note No. 437.
Kain, J.S., Fritsch, J.M., 1993. Convective parameterization for mesoscale models: the Kain-Fritsch scheme. The representation of cumulus convection in numerical models, Meteor. Monogr. No. 46 Am. Meteor. Soc. 165–170.
Kain, J.S., 2004. The Kain-Fritsch convective parameterization: an update. J. Appl. Meteor 43, 170–181.
Kalnay, E., et al., 1996. The NCEP/NCAR reanalysis 40-year project. Bull. Am. Meteor. Soc. 77, 437–471.
Kotroni, V., Lagouvardos, K., 2001. Precipitation forecast skill of different convective parameterization and microphysical schemes: application for the cold season over Greece. Geophys. Res. Lett. 28, 1977–1980.
Kotroni, V., Lagouvardos, K., 2004. Evaluation of MM5 high-resolution real-time forecasts over the urban area of Athens, Greece. J. Appl. Meteor 43, 1666–1678.
Kotroni, V., Lagouvardos, K., 2008. Lightning occurrence in relation with elevation, terrain slope and vegetation cover in the Mediterranean. JGR-Atmospheres 133, D21118.
Lagouvardos, K., Kotroni, V., Betz, H.D., Schmidt, K., 2009. A comparison of lightning data provided by ZEUS and LINET networks over Western Europe. Nat. Hazards Earth Syst. Sci. 9, 1713–1717.
Lagouvardos, K., Kotroni, V., Defer, E., Bousquet, O., 2013. Study of a heavy precipitation event over southern France, in the frame of HYMEX project: observational analysis and model results using assimilation of lightning. Atmos. Res. 134, 45–55.
Liu, J., Bray, M., Han, D., 2012. Sensitivity of the weather research and forecasting (WRF) model to downscaling ratios and storm types in rainfall simulation. Hydrol. Process 26, 3012–3031.
Lynn, B., Kelman, G., Ellrod, G., 2015. An evaluation of the efficacy of using observed lightning to improve convective lightning forecasts. Weather Forecast. 30, 405–423.
Mansell, E.R., Ziegler, C.L., MacGorman, D.R., 2007. A lightning data assimilation technique for mesoscale forecast models. Mon. Weather Rev. 135, 1732–1748.
Margvelashvili, N., Andrewartha, J., Herzfeld, M., Robson, B.J., Brandon, V.E., 2013. Satellite data assimilation and estimation of a 3D coastal sediment transport model using error-subspace emulators. Env. Mod. Softw. 40, 191–201.
Mazarakis, N., Kotroni, V., Lagouvardos, K., Argiriou, A.A., 2009. The sensitivity of numerical forecasts to convective parameterization during the warm period and the use of lightning data as an indicator for convective occurrence. Atmos. Res. 94, 704–714.
Mlawer, E.J., Taubman, S.J., Brown, P.D., Iacono, M.J., Clough, S.A., 1997. Radiative transfer for inhomogeneous atmosphere: RRTM, a validated correlated-k model for the longwave. J. Geophys. Res. 102 (D14), 166663–166682.
Papadopoulos, A., Chronis, T.G., Anagnostou, E.N., 2005. Improving convective precipitation forecasting through assimilation of regional lightning measurements in a mesoscale model. Mon. Weather Rev. 133, 1961–1977.
Papadopoulos, A., Serpetzoglou, E., Anagnostou, E.N., 2009. Evaluating the impact of lightning data assimilation on mesoscale model simulations of a flash flood inducing storm. Atmos. Res. 94, 715–725.
Pessi, A.T., Businger, S., 2009. The impact of lightning data assimilation on a winter storm simulation over the North Pacific ocean. Mon. Weather Rev. 137, 3177–3195.
Peters-Lidard, C.D., Kemp, E.M., Matsui, T., Santanello Jr., J.A., Kumar, S.V., Jacob, J.P., Clune, T., Tao, W.-K., Chin, M., Hou, A., Case, J.L., Kim, D., Kim, K.-M., Lau, W., Liu, Y., Shi, J., Starr, D., Tan, Q., Tao, Z., Zaitchik, B.F., Zavodsky, B., Zhang, S.Q., Zupanski, M., 2015. Integrated modeling of aerosol, cloud, precipitation and land processes at satellite-resolved scales. Env. Mod. Softw. 67, 149–159.
Qie, X., Zhu, R., Yuan, T., Wu, X., Li, W., Liu, D., 2014. Application of total-lightning data assimilation in a mesoscale convective system based on the WRF model. Atmos. Res. 145–146, 255–266.
Rodgers, R.F., Fritsch, J.M., Lambert, W.C., 2000. A simple technique for using radar data in the dynamic initialization of a mesoscale model. Mon. Weather Rev. 128, 2560–2574.
Schultz, C.J., Petersen, W.A., Carey, L.D., 2011. Lightning and severe weather: a comparison between total and cloud-to-ground lightning trends. Weather Forecast. 26, 744–755.
Skamarock, W.C., Klemp, J.B., Dudhia, J., Gill, D.O., Barker, D.M., Duda, M.G., Huang, X.Y., Wang, W., Powers, J.G., 2008. A Description of the Advanced Research WRF Version 3. NCAR Technical Note, NCAR/TN-475+STR, June 2008, Boulder Colorado, USA, p. 125.
Thompson, G., Field, P.R., Rasmussen, R.M., Hall, W.D., 2008. Explicit forecasts of winter precipitation using an improved bulk microphysics scheme. Part II: implementation of a new snow parameterization. Mon. Weather Rev. 136, 5095–5115.
Van Loon, M., Builtjes, P.J.H., Segers, A.J., 2000. Data assimilation of ozone in the atmospheric transport chemistry model LOTOS. Env. Mod. Softw. 15, 603–609.
Wilks, D.S., 1995. Statistical Methods in the Atmospheric Sciences. Academic Press, p. 467.
Zhou, Y., Qie, X., Soula, S., 2002. A study of the relationship between cloud-to-ground lightning and precipitation in the convective weather system in China. Ann. Geophys. 20, 107–113.